arXiv:1612.07173v1 [cond-mat.quant-gas] 21 Dec 2016

Evidence for Griffiths-Type Dynamics near the Many-Body Localization Transition in Quasi-Periodic Systems

Henrik P. Lüschen,[1,2] Pranjal Bordia,[1,2] Sebastian Scherg,[1,2] Fabien Alet,[3] Ehud Altman,[4,5] Ulrich Schneider,[1,2,6] and Immanuel Bloch[1,2]

[1] *Fakultät für Physik, Ludwig-Maximilians-Universität München, Schellingstr. 4, 80799 Munich, Germany*
[2] *Max-Planck-Institut für Quantenoptik, Hans-Kopfermann-Str. 1, 85748 Garching, Germany*
[3] *Laboratoire de Physique Théorique, IRSAMC, Université de Toulouse, CNRS, 31062 Toulouse, France*
[4] *Department of Condensed Matter Physics, Weizmann Institute of Science, Rehovot 7610001, Israel*
[5] *Department of Physics, University of California, Berkeley, CA 94720*
[6] *Cavendish Laboratory, University of Cambridge, Cambridge CB3 0HE, UK*

(Dated: December 22, 2016)

In the presence of sufficiently strong disorder an interacting many-body system can fail to thermalize and become many-body localized. However, already below the many-body localization transition, thermalization can be strongly impeded by rare, already localized regions. In this work, we experimentally and numerically observe signatures of these so-called Griffiths regions in a quasi-periodic system. Here, unlike in systems with true-random disorder, rare localized regions cannot result from the disorder pattern alone, but instead emerge due to randomness in the initial state. Specifically, we observe a power-law decay of an initial charge-density wave pattern on intermediate timescales, which has been predicted for the Griffiths regime. From this decay, we are able to access the dynamical exponent and find evidence for an extended sub-diffusive regime.

Introduction.— An isolated quantum system of interacting particles can be non-ergodic and fail to thermalize in the presence of sufficiently strong disorder [1–14]. This phenomenon – called many-body localization (MBL) – presents a generic alternative to thermalization [15–17] and has attracted an immense amount of interest in recent years, see e.g. Refs. [8, 9] for reviews. More recently, theoretical studies started to address the transition from the thermalizing to the MBL phase itself (reviewed in Refs. [18–20]). This transition is of particular interest, since, in contrast to conventional quantum phase transitions [21], which occur only in the ground state, the MBL transition happens over a wide range of energy densities. Furthermore, a good understanding of the transition may give new insight into thermalization in closed quantum systems [22]. However, numerical methods such as exact diagonalization (ED) and tensor network methods, which efficiently work in the MBL regime, struggle close to the transition, as the relevant lengthscale(s) become much larger than the numerically tractable system sizes and the system becomes highly entangled. Experiments can overcome these limitations and hence promise to give new insights into the transition.

Recently, an effective theory of the transition in true-random spin systems was developed based on renormalization group (RG) schemes [23, 24]. In analogy to conventional quantum phase transitions, a single diverging lengthscale ξ was found to emerge when approaching the transition from the thermal side. Within the RG, this correlation length diverges at the critical disorder strength Δ_c^{MBL} as $\xi \sim |\Delta - \Delta_c^{\mathrm{MBL}}|^{-\nu}$, with a supposedly universal scaling exponent $\nu \approx 3$. Close to the transition, however, a Griffiths regime [25] is predicted, in which the dynamics is dominated by rare, locally critical or insulating inclusions in the thermalizing bulk of the system. Such regions have been suggested to appear with a probability density $p(L) \sim (1/\xi)e^{-L/\xi}$, where $p(L)$ represents the probability that a given site is part of an inclusion of length L. These critical inclusions will eventually be thermalized by their thermal surroundings on a timescale $\tau \sim e^{L/x_0}$, where x_0 is a non-critical microscopic lengthscale [23, 24]. Employing these relations, the exponential distribution of rare region sizes translates to a broad power-law distribution of relaxation times τ in the system: $p(\tau) \sim (1/\tau)^{1+1/z}$, with $z = \xi/x_0$. This distribution dictates the decay of global density patterns, such as e.g. an initial charge-density wave [13]. The residual deviation from equilibrium, quantified by the density imbalance $\mathcal{I}(t)$, is proportional to the fraction of sites that have not yet thermalized because they belong to inclusions with $\tau > t$, yielding a power-law decay of the imbalance:

$$\mathcal{I}(t) \sim \int_t^\infty p(\tau)\, d\tau \sim t^{-1/z}, \tag{1}$$

As discussed in Refs. [23, 24], z denotes the dynamical exponent associated with transport. In contrast to conventional metal-insulator phase transitions, where transport remains diffusive ($1/z = 0.5$), at the MBL transition $1/z$ vanishes continuously on approaching the critical point (Fig. 1a), indicating a regime with sub-diffusive transport. Numerical studies have supported this idea by finding slow power-law relaxation processes [26–30]. Regarding scaling close to the transition, however, ED studies find a universal exponent of $\nu \approx 1$ [31, 32] in disagreement with RG-studies and violating the Harris-Chayes [33–35] criterion, which places a lower bound of $\nu \geq 2$ on the critical exponent in disordered systems.

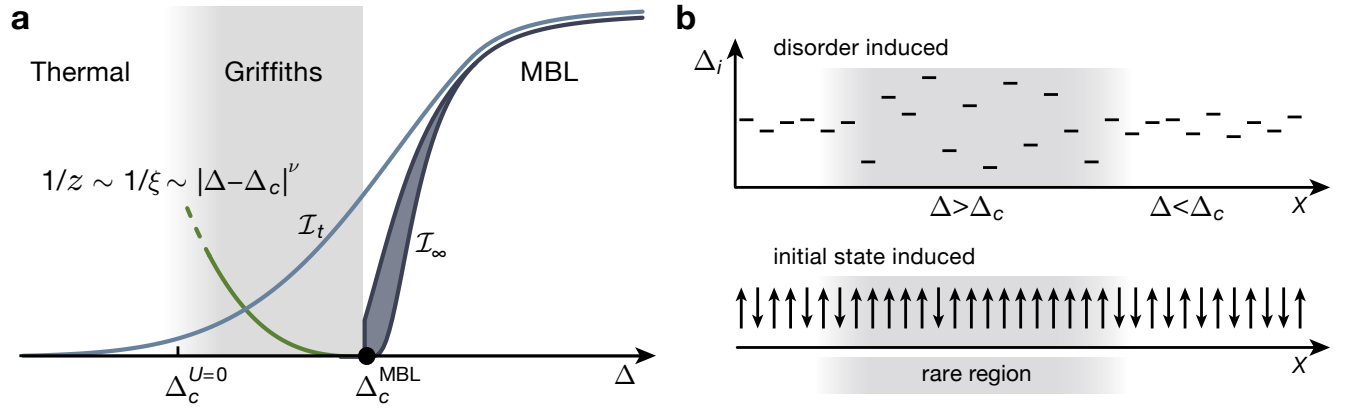

FIG. 1. **Schematic of Griffiths regions below the MBL critical point:** a) Behavior of the density imbalance $\mathcal{I}$ between even and odd sites of an initially prepared density pattern across the MBL transition at Δ_c^{MBL}. While the precise behavior of the imbalance at infinite times $\mathcal{I}_\infty$ just above the critical point is still unclear, it is finite only in the many-body localized phase. At finite times t, however, a finite imbalance $\mathcal{I}_t$ can also occur on the ergodic side, due to some rare regions thermalizing very slowly. Those regions eventually become thermalized by the surrounding system on very long timescales, which gives rise to a Griffiths regime (gray shading) of slow dynamics below the MBL phase. These slow dynamics follow a power-law decay $\mathcal{I}(t) \sim t^{-1/z}$, where z denotes the varying dynamical exponent. At the MBL transition, $1/z$ should continuously approach zero [23, 24]. Below the single particle localization transition at $\Delta_c^{U=0}$, locally critical or insulating regions cannot exist, as single particles can delocalize individually. b) Rare critical or insulating regions immersed in an otherwise thermal system can be caused via two mechanisms: Disorder induced regions appear due to a locally larger disorder strength Δ in true-random disorder. Initial state induced regions are e.g. caused by fluctuations in the local spin-density. This creates effectively non-interacting regions, which are initially insulating above the single-particle localization transition.

Far less is known about the transition in systems with quasi-periodic potentials. While the existence of MBL in this case is well supported by both numerics [36] and experiments [13], the existence of a Griffiths regime has been challenged due to the a priori absence of statistically rare regions in a deterministic quasi-periodic potential [37].

In this work, we experimentally and numerically investigate the regime below the MBL transition in a fermionic, quasi-periodic Hubbard model. On intermediate timescales, we find evidence for a Griffiths regime with slow relaxation dynamics, reminiscent of systems with true-random disorder. Specifically, we find a regime consistent with power-law decaying imbalances, the exponent of which continuously decreases when approaching the transition. We attribute this to a random distribution of atoms and spins in the initial state, which causes Griffiths regions due to the particle- and spin-density dependence of the MBL critical disorder strength (Fig. 1). For example, a rare region containing only a single spin species would be non-interacting and therefore behave insulating above the single-particle localization transition (Fig. 1b).

Experiment.— Our experimental setup effectively implements the interacting Aubry-André model [36, 38], which describes spinful fermions on a lattice with nearest neighbor tunneling of amplitude $J \approx h \times 500\,\mathrm{Hz}$ and on-site interactions of strength U. The fermions are subjected to a quasi-periodic correlated disorder potential of the form $\Delta \cos(2\pi\beta i + \phi)$, where Δ and ϕ denote the strength and relative phase of the potential, i numbers the lattice site and the irrational β gives the disorder periodicity (see [39] for details). This model has a localization transition at $\Delta_c^{U=0} = 2J$ in the absence of interactions [38], and was shown to exhibit MBL above a critical disorder strength [13].

We prepare a high energy initial charge-density wave (CDW) state, where up and down spin atoms are randomly distributed on even lattice sites, while odd lattice sites are empty. During the preparation, doubly occupied lattice sites are suppressed by strong repulsive interactions. The CDW in the central tube is approximately 200 sites long and contains about 80 atoms. In contrast to previous experiments [13], in this work we only mildly confine the atom cloud during the ensuing time evolution in order to reduce the effects of the overall harmonic trapping potential. After a variable evolution time, we extract the imbalance $\mathcal{I} = (N_\mathrm{e} - N_\mathrm{o})/(N_\mathrm{e} + N_\mathrm{o})$ between the populations of even (N_e) and odd (N_o) sites using a band mapping technique [40]. The imbalance has an initial value close to one and in a thermal system will ultimately decay to zero. In contrast, a finite imbalance indicates a memory of the initial state, and signals that the system has not fully thermalized yet. Since the imbalance is a local probe and does not require global mass transport to relax, it exhibits a short intrinsic relaxation timescale of $\mathcal{O}(\tau)$ in the non-disordered case, where $\tau = \hbar/J$ is the tunneling time. This allows for an experimental discrimination of slow, disorder induced

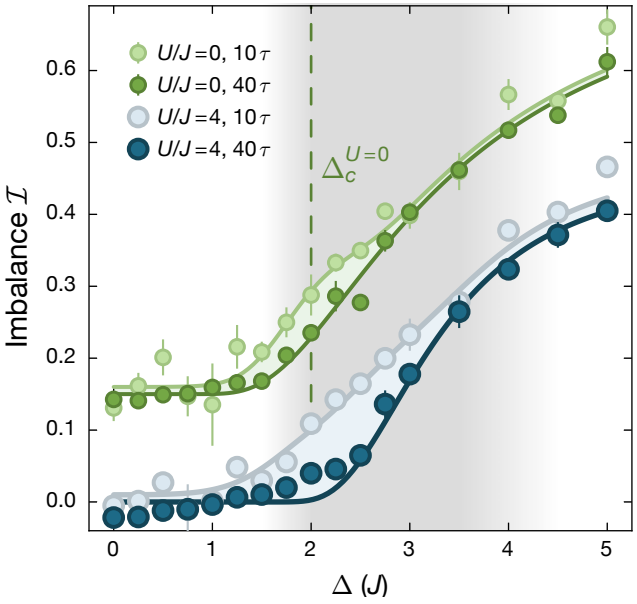

FIG. 2. **Imbalance at finite times:** Measurements of the imbalance $\mathcal{I}$ after $10\,\tau$ (light points) and $40\,\tau$ (dark points) for the non-interacting system and at $U = 4\,J$. The non-interacting data is vertically offset by 0.15 for clarity. The data represents averages over 12 disorder phases ϕ with errorbars indicating the uncertainty of the mean. Solid lines are guides to the eye. In the interacting system, we observe a regime (gray shaded), where the imbalance after $40\,\tau$ is significantly lower than after $10\,\tau$, indicating a dynamical evolution of the system. A similar, but much less pronounced, feature is also present in the non-interacting case.

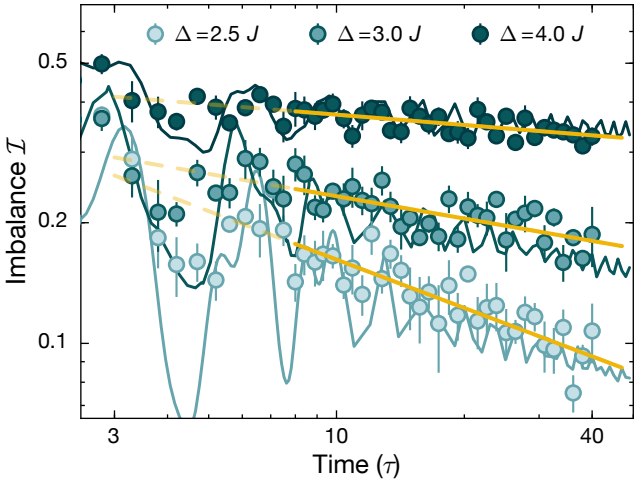

FIG. 3. **Time evolution of the imbalance close to the MBL transition**: Decay of an initially prepared charge-density wave at a fixed interaction strength of $U = 4\,J$ for various disorder strengths Δ. Points mark experimental data, averaged over six disorder phases ϕ, with errorbars indicating the uncertainty of the mean. The corresponding ED simulations for $S = 16$ sites [39] are indicated as solid lines of the same color. During the first three tunneling times (not shown), the imbalance quickly decays from its initial value close to one. During this initial decay, the imbalance shows strong oscillations, which cease after $\sim 8\,\tau$. Thereafter, we observe a much slower further decay, which is consistent with a power-law (yellow lines are power-law fits).

dynamics. In contrast, global observables are expected to show hydrodynamic tails in the ergodic phase [41], which would mask the slow relaxation processes. For details of the setup and the experimental sequence, see Refs. [13, 39].

Finite-Time Imbalance.— Fig. 2 shows measurements of the imbalance at various disorder strengths Δ for both the non-interacting case and at an interaction strength of $U = 4\,J$. The measurements were taken after $10\,\tau$ (called short), which is nonetheless long enough for a clean system to relax, and after $40\,\tau$ (called long). We refrain from accessing imbalances at times longer than $40\,\tau$, since then background decays, which limit the lifetime of the imbalance to $\mathcal{O}(10^3\,\tau)$, become increasingly relevant [39, 42, 43].

From the interacting data we can distinguish three different regimes, as is indicated by the gray background shading. In the regimes of weak ($\Delta \lesssim 1.5\,J$) and strong ($\Delta \gtrsim 4\,J$) disorder, the imbalances measured after short and long times agree up to the effect of background decays [39, 42, 43]. The weak disorder regime is thermal, with the imbalance quickly relaxing to zero, the strong disorder regime shows many-body localization indicated by a rapid approach of the imbalance to a finite stationary value. In the gray shaded regime of intermediate disorder strength ($1.5\,J \lesssim \Delta \lesssim 4\,J$), we observe a significant difference between the interacting short and long term imbalance, indicating the presence of relaxation dynamics on a slow timescale. A similar trend also exists in the non-interacting case. However, it is much less pronounced, suggesting that interactions give rise to a thermalization mechanism even when all single-particle states are localized. In the following, we present a detailed experimental characterization of the slow dynamics in the interacting system. This will allow us to identify a Griffiths regime and estimate the location of the critical point more precisely than is possible via the finite time imbalances.

Imbalance Time Traces.— We perform a closer investigation of the slow dynamics in the interacting system by monitoring the time evolution of the imbalance for various disorder strengths above the non-interacting transition (see Fig. 3). The imbalance is plotted for times between $3-40\,\tau$, which omits the rapid initial decay from its starting value close to one [13]. In between $10-40\,\tau$, we observe slow decays of the imbalance, which are consistent with a power law behavior $\mathcal{I}(t) \sim t^{-1/z}$. This behavior is well reproduced by ED simulations shown in Fig. 3, which model our system on 16 sites [39]. In

spin models with true-random disorder, such power-law decays result from rare, locally critical or insulating regions immersed in an otherwise thermal system. In true-random systems, such rare regions emerge due to (i) statistical spatial variations in the disorder strength and (ii) local variations in the initial state [29] (see Fig. 1b). Specifically, a true-random distribution of on-site energies will result in subregions with a locally higher (lower) disorder strength, which form locally insulating (thermalizing) regions. Similarly, a random initial state with fixed average spin-density will show regions with different local spin-densities. These regions will localize at different disorder strengths, as the MBL critical point changes with particle and spin density. The deterministic quasi-periodic potential in our system does not allow for mechanism (i), however, random spatial fluctuations in the initial state are present in our system and induce rare regions which could lead to Griffiths physics through mechanism (ii). While the long time fate of such initial state induced Griffiths effects has not been analyzed yet, here we assume that, on the time scales of the experiment, we can analyze them in the same way as disorder induced Griffiths phenomena.

Relaxation Exponent.— We extract the exponents of the observed power-laws via linear fits of $\log(\mathcal{I})$ versus $\log(t)$ between $8-40\,\tau$ to the experimental data, see Fig. 4. The experimental values are compared to the result of our ED simulations, where we choose a fitting range of $20-80\,\tau$, as initial oscillations in the imbalance cease slower than in the experiment and affect the fitted exponent [39]. We show exponents only for $\Delta \geq 2\,J$ as below the single-particle transition, locally insulating regions cannot exist, since every particle can delocalize individually. Hence, we also do not expect a power-law type decay, and indeed find poorly converging fits in this regime [39]. This is in stark contrast to models with true-random disorder, where single-particle states are localized even at infinitesimal disorder strengths [44] and the effects of rare regions could remain important even at low disorder strengths [29, 30, 45]. Just above the single-particle localization transition, we observe a value of $1/z \approx 0.5$, compatible with a diffusive behavior. Upon further increasing the disorder strength, $1/z$ decreases monotonically, indicating a sub-diffusive regime, in which the dynamics is affected by locally critical or insulating regions of increasing size. In this regime, we find good agreement between experiment and ED, suggesting that the correlation length ξ, and hence the size of typical rare-regions relaxing on the experimental timescales, are smaller than the simulated system size of 16 sites. Eventually, the experimental values of $1/z$ saturate at a non-zero offset z_o^{-1}. We have checked that this offset is consistent with the expected effect of background decays in our system [39, 42, 43], suggesting that $1/z$ could indeed vanish at the transition. We note that also on the MBL side there may be a regime of slow, logarithmic relaxation towards the stationary value of the imbalance [46]. During the moderate times accessed in this study, such a slow logarithmic relaxation might also contribute to the finite value of z_o^{-1}. The ED calculations also likely fail to pinpoint the transition, as the correlation length becomes larger than the system size used for the simulations.

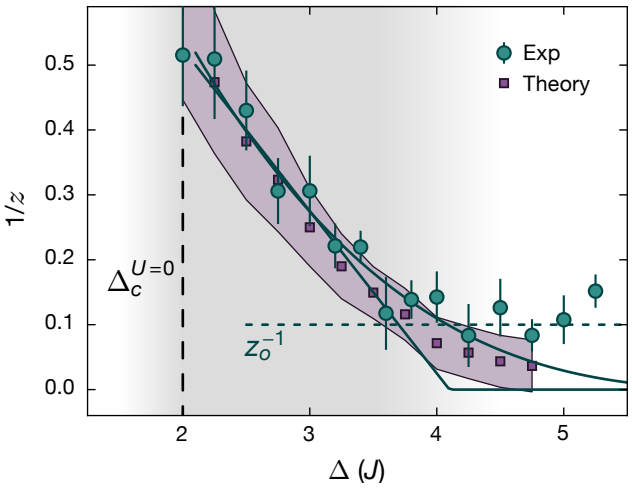

FIG. 4. **Power-law exponent of imbalance decay:** Experimental and theoretical (ED, $S = 16$, see [39]) fitted exponents $1/z$ of the power-law decay as a function of disorder strength Δ at a fixed interaction strength of $U = 4\,J$. Errorbars indicate the uncertainty of the fit to the experimental data. The purple shading denotes an estimate of the uncertainty on the simulated exponents, which is dominantly due to finite size effects [39]. The gray shading marks the regime of slow dynamics as observed in Fig 2. Below the single-particle localization transition at $\Delta_c^{U=0}$ (black dashed line), we do not expect power-law decays, as rare regions cannot exist in a regime where single particles can delocalize individually. At large disorder strengths, the experimental value saturates at a non-zero offset z_o^{-1}, consistent with the independently observed background lifetime [39, 42, 43]. The finite value of $1/z$ in ED for large disorder strength is likely caused by finite size effects. The solid lines indicate possible universal scalings according to $1/z \sim |\Delta - \Delta_c^{\mathrm{MBL}}|^\nu$ with exemplary universal exponents of $\nu = 3$ (upper line) and $\nu = 1$ (lower line).

Close to the transition, $1/z$ is expected to show a universal dependence according to $1/z \sim \xi^{-1} \sim |\Delta - \Delta_c^{\mathrm{MBL}}|^\nu$ [23, 24] for true-random disorder. However, from our data it is not possible to access this critical scaling regime, as the background decay masks the behavior close to the transition and the scaling behavior might not be valid further away from the transition. Additionally, it is not a priori clear whether the observed power-law decay of the state induced rare regions will persist to all times, as the initial state will be rearranged when the system thermalizes, especially in the presence of a mobile spin-sector [47]. In Fig. 4 we show two exemplary critical scalings with exponents of $\nu = 3$ and $\nu = 1$ respectively. We find

that both behaviors would be consistent with our data. Additionally, the two scalings give different values of Δ_c^{MBL}, and hence we are not able to precisely pinpoint the location of the phase transition point.

Conclusion.— We have experimentally observed slow, interaction-induced relaxation dynamics close to the MBL phase transition in the Aubry-André model, in very good agreement with ED simulations. Specifically, we observe a decay of an initial charge-density wave, which is consistent with a power-law and hence reminiscent of dynamics predicted and found in spin models with true-random disorder [23, 24, 26–29] attributed to rare Griffiths regions. While such dynamics has been argued not to exist in quasi-periodic systems [37], they can emerge from randomness in the initial state and a spin density dependent transition point, a mechanism that is also relevant to spin models [29]. From our data, we can extract the dynamical exponent $1/z$, which we find to continuously decrease when approaching the transition, indicating the presence of a sub-diffusive regime. However, finite couplings to the environment prevent us from precisely pinpointing the location of the transition or extracting accurate values for the universal exponent ν.

Future works could address the problem of a finite bath coupling via a systematic analysis of its effects [43]. This could also allow addressing the question of the long term fate of initial state induced rare regions. In addition, the suggested mechanism for the creation of rare regions could be tested by e.g. loading initial states with different entropies. A similar study would also be interesting in the presence of true-random disorder, where the dynamics in the weak-disorder regime could be investigated [29, 30, 45]. Another interesting direction is the investigation of Griffiths effects in higher dimensional and Floquet MBL systems [37, 48, 49].

Acknowledgments.— We acknowledge useful discussions with Eugene Demler, Michael Knap and Christophe Salomon. We acknowledge financial support by the European Commission (UQUAM, AQuS) and the Nanosystems Initiative Munich (NIM). This work benefited from the support of the project THERMOLOC ANR-16-CE30-0023-02 of the French National Research Agency (ANR). ED simulations were performed using HPC resources from GENCI (grant x2016050225) and CALMIP (grant 2016-P0677).

[1] D.M. Basko, I. L. Aleiner, and B. L. Altschuler, "Metal-insulator transition in a weakly interacting many-electron system with localized single-particle states," Ann. Phys. **321** (2006).

[2] I. V. Gornyi, A. D. Mirlin, and D. G. Polyakov, "Interacting electrons in disordered wires: Anderson localization and low-t transport," Phys. Rev. Lett. **95**, 206603 (2005).

[3] John Z. Imbrie, "On many-body localization for quantum spin chains," Journal of Statistical Physics **163**, 998–1048 (2016).

[4] V. Oganesyan and D. A. Huse, "Localization of interacting fermions at high temperature," Phys. Rev. B **75**, 155111 (2007).

[5] A. Pal and D. A. Huse, "Many-body localization phase transition," Phys. Rev. B **82**, 174411 (2010).

[6] R. Vosk and E. Altman, "Many-body localization in one dimension as a dynamical renormalization group fixed point," Phys. Rev. Lett. **110**, 067204 (2013).

[7] V. P. Michal, I. L. Aleiner, B. L. Altshuler, and G. V. Shlyapnikov, "Finite-temperature fluidinsulator transition of strongly interacting 1d disordered bosons," PNAS **113**, E4455–E4459 (2016).

[8] R. Nandkishore and D. A. Huse, "Many-body localization and thermalization in quantum statistical mechanics," Annu. Rev. Condens. Matter Phys. **6**, 15–38 (2015).

[9] E. Altman and R. Vosk, "Universal dynamics and renormalization in many-body-localized systems," Annu. Rev. Condens. Matter Phys. **6**, 383–409 (2015).

[10] Y. Bahri, R. Vosk, E. Altman, and A. Vishwanath, "Localization and topology protected quantum coherence at the edge of hot matter," Nat. Commun. **6** (2015).

[11] M. Serbyn, M. Knap, S. Gopalakrishnan, Z. Papić, N. Y. Yao, C. R. Laumann, D. A. Abanin, M. D. Lukin, and E. A. Demler, "Interferometric probes of many-body localization," Phys. Rev. Lett. **113**, 147204 (2014).

[12] M. Ovadia, D. Kalok, I. Tamir, S. Mitra, B. Sacépé, and D. Shahar, "Evidence for a finite-temperature insulator," Scientific Reports **5** (2015).

[13] M. Schreiber, S. S. Hodgman, P. Bordia, H. P. Lüschen, M. H. Fischer, R. Vosk, E. Altman, U. Schneider, and I. Bloch, "Observation of many-body localization of interacting fermions in a quasirandom optical lattice," Science **349**, 842–845 (2015).

[14] J. Smith, A. Lee, P. Richerme, B. Neyenhuis, P. W. Hess, P. Hauke, M. Heyl, D. A. Huse, and C. Monroe, "Many-body localization in a quantum simulator with programmable random disorder," Nat Phys **12**, 907–911 (2016).

[15] J. M. Deutsch, "Quantum statistical mechanics in a closed system," Phys. Rev. A **43**, 2046–2049 (1991).

[16] M. Srednicki, "Chaos and quantum thermalization," Phys. Rev. E **50**, 888–901 (1994).

[17] M. Rigol, V. Dunjko, and M. Olshanii, "Thermalization and its mechanism for generic isolated quantum systems," Nature **452** (2008).

[18] S. A. Parameswaran, A. C. Potter, and R. Vasseur, "Eigenstate phase transitions and the emergence of universal dynamics in highly excited states," (2016), arXiv:1610.03078.

[19] D. J. Luitz and Y. Bar Lev, "The ergodic side of the many-body localization transition," (2016), arXiv:1610.08993.

[20] K. Agarwal, E. Altman, E. Demler, S. Gopalakrishnan, D. A. Huse, and M. Knap, "Rare region effects and dynamics near the many-body localization transition," (2016), arXiv:1611.00770.

[21] S. Sachdev, *Quantum Phase Transitions* (Cambridge University press, 2001).

[22] D. J. Luitz and Y. Bar Lev, "Anomalous thermalization

in ergodic systems," Phys. Rev. Lett. **117**, 170404 (2016).
[23] R. Vosk, D. A. Huse, and E. Altman, "Theory of the many-body localization transition in one-dimensional systems," Phys. Rev. X **5**, 031032 (2015).
[24] A. C. Potter, R. Vasseur, and S. A. Parameswaran, "Universal properties of many-body delocalization transitions," Phys. Rev. X **5**, 031033 (2015).
[25] R. B. Griffiths, "Nonanalytic behavior above the critical point in a random ising ferromagnet," Phys. Rev. Lett. **23**, 17–19 (1969).
[26] K. Agarwal, S. Gopalakrishnan, M. Knap, M. Müller, and E. Demler, "Anomalous diffusion and griffiths effects near the many-body localization transition," Phys. Rev. Lett. **114**, 160401 (2015).
[27] Y. Bar Lev, G. Cohen, and D. R. Reichman, "Absence of diffusion in an interacting system of spinless fermions on a one-dimensional disordered lattice," Phys. Rev. Lett. **114**, 100601 (2015).
[28] E. J. Torres-Herrera and Lea F. Santos, "Dynamics at the many-body localization transition," Phys. Rev. B **92**, 014208 (2015).
[29] D. J. Luitz, N. Laflorencie, and F. Alet, "Extended slow dynamical regime close to the many-body localization transition," Phys. Rev. B **93**, 060201 (2016).
[30] M. Žnidarič, A. Scardicchio, and V. K. Varma, "Diffusive and subdiffusive spin transport in the ergodic phase of a many-body localizable system," Phys. Rev. Lett. **117**, 040601 (2016).
[31] J. A. Kjäll, J. H. Bardarson, and F. Pollmann, "Many-body localization in a disordered quantum ising chain," Phys. Rev. Lett. **113**, 107204 (2014).
[32] D. J. Luitz, N. Laflorencie, and F. Alet, "Many-body localization edge in the random-field heisenberg chain," Phys. Rev. B **91**, 081103 (2015).
[33] A. B. Harris, "Effect of random defects on the critical behaviour of ising models," J. Phys. Condens. **7**, 1671 (1974).
[34] J. T. Chayes, L. Chayes, D. S. Fisher, and T. Spencer, "Finite-size scaling and correlation lengths for disordered systems," Phys. Rev. Lett. **57**, 2999–3002 (1986).
[35] A. Chandran, C. R. Laumann, and V. Oganesyan, "Finite size scaling bounds on many-body localized phase transitions," (2015), arXiv:1509.04285.
[36] S. Iyer, V. Oganesyan, G. Refael, and D. A. Huse, "Many-body localization in a quasiperiodic system," Phys. Rev. B **87**, 134202 (2013).
[37] S. Gopalakrishnan, K. Agarwal, E. A. Demler, D. A. Huse, and M. Knap, "Griffiths effects and slow dynamics in nearly many-body localized systems," Phys. Rev. B **93**, 134206 (2016).
[38] S. Aubry and G. André, "Analyticity breaking and anderson localization in incommensurate lattices," Ann. Israel Phys. Soc. **3** (1980).
[39] See Supplementary Material for details.
[40] S. Trotzky, Y-A. Chen, A. Flesch, I. P. McCulloch, U. Schollwöck, J. Eisert, and I. Bloch, "Probing the relaxation towards equilibrium in an isolated strongly correlated one-dimensional bose gas," Nat. Phys. **8** (2012).
[41] J. Lux, J. Müller, A. Mitra, and A. Rosch, "Hydrodynamic long-time tails after a quantum quench," Phys. Rev. A **89**, 053608 (2014).
[42] P. Bordia, H. P. Lüschen, S. S. Hodgman, M. Schreiber, I. Bloch, and U. Schneider, "Coupling identical one-dimensional many-body localized systems," Phys. Rev. Lett. **116**, 140401 (2016).
[43] H. P. Lüschen, P. Bordia, S. S. Hodgman, M. Schreiber, S. Sarkar, A. J. Daley, M. H. Fischer, E. Altman, I. Bloch, and U. Schneider, "Signatures of many-body localization in a controlled open quantum system," (2016), arXiv:1610.01613.
[44] P. W. Anderson, "Absence of diffusion in certain random lattices," Phys. Rev. **109**, 1492–1505 (1958).
[45] I. Khait, S. Gazit, N. Y. Yao, and A. Auerbach, "Spin transport of weakly disordered heisenberg chain at infinite temperature," Phys. Rev. B **93**, 224205 (2016).
[46] M. Mierzejewski, J. Herbrych, and P. Prelovšek, "Universal dynamics of density correlations at the transition to many-body localized state," (2016), arXiv:1607.04992.
[47] P. Prelovšek, O. S. Barišić, and M. Žnidarič, "Absence of full many-body localization in the disordered Hubbard chain," Phys. Rev. B **94**, 241104 (2016).
[48] J.-y. Choi, S. Hild, J. Zeiher, P. Schauß, A. Rubio-Abadal, T. Yefsah, V. Khemani, D. A. Huse, I. Bloch, and C. Gross, "Exploring the many-body localization transition in two dimensions," Science **352**, 1547–1552 (2016).
[49] P. Bordia, H. P. Lüschen, U. Schneider, M. Knap, and I. Bloch, "Periodically driving a many-body localized quantum system," (2016), arXiv:1607.07868.
[50] C. A. Regal, C. Ticknor, J. L. Bohn, and D. S. Jin, "Creation of ultracold molecules from a fermi gas of atoms," Nature **424** (2003).
[51] V. Hernandez, J. E. Roman, and V. Vidal, "SLEPc: A scalable and flexible toolkit for the solution of eigenvalue problems," ACM Trans. Math. Software **31**, 351–362 (2005).

Supplementary Material

Comparison to the non-interacting system

We perform a detailed comparison of the interacting and non-interacting slow relaxation dynamics shown in Fig. 2. Fig. S1 compares the imbalance time traces for disorder strengths below and close to the non-interacting transition point ($\Delta_c^{U=0} = 2\,J$), as well as below and close to the estimated interacting transition. The data omits the fast initial decay of the imbalance, and shows a slow, further decay in the time window spanned by the 'short' ($10\,\tau$) and 'long' ($40\,\tau$) observation times of Fig. 2. Below and close to the non-interacting transition at $\Delta_c^{U=0} = 2\,J$, the imbalance has quickly reached rather low values and shows strong fluctuations in the further decay. Above the non-interacting transition, we observe power-law decays emerging in the interacting case, while the non-interacting system is localized. At even larger disorder strengths, presumably above the many-body localization transition, both the interacting and the non-interacting system only show a slow residual decay due to external couplings.

These observations are consistent with the following picture: Below $\Delta_c^{U=0}$, even single particles are not localized and we observe a similar behavior with and without interactions. While non-interacting particles will spread slower close to their localization transition at $\Delta_c^{U=0}$, and hence the relaxation becomes slower, we do not expect this relaxation to follow a power-law. Instead, the dynamics should continue to exhibit oscillations with a decaying envelope. In the experiment these oscillations dephase much quicker than in numerical simulations, as the experimental imbalances are averaged over many 1D tubes with slightly different tunneling rates J [13]. As shown in Fig. S2, the resulting trend still resembles a linear behavior on a log-log scale for the experimentally relevant times. Similar arguments also hold for disorder strengths at, or just above the non-interacting transition, as particles have not managed to spread to their single-particle localization length within the times accessed in our experiment. Hence, also in this regime, the observed dynamics of both the interacting and non-interacting system are similar for short times.

Only when the disorder strength is high enough to restrict the single-particle dynamics ($\Delta \gtrsim 2.5\,J$) to a sufficiently short localization length, clean power-law decays emerge in the interacting system (see also Fig.3). At even larger disorder strengths, the interacting and non-interacting data look alike again, as both systems are presumably localized. In this regime, the interacting imbalance still decays slightly faster than its non-interacting equivalent, as the effects of external bath couplings are larger in the presence of interactions [42, 43]. Additionally, an intermediate logarithmic relaxation might also

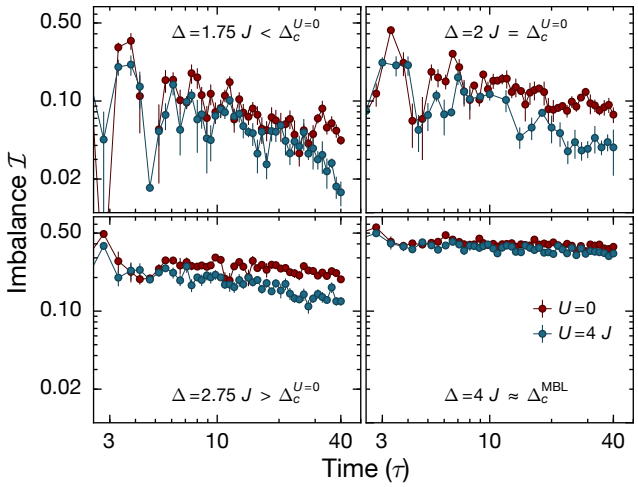

FIG. S1. **Interacting vs. non-interacting time traces:** Comparison between the decay of an initially prepared charge-density wave in the absence and presence of interactions for various disorder strengths Δ. Each point is the average over 6 disorder phases ϕ, with errorbars indicating the uncertainty of the mean. During the first three tunneling times (not shown), the imbalance quickly decays from its initial value close to one before the dynamics crosses over into the shown, much slower regime.

be present in the MBL phase [46].

Still, a naive evaluation of the non-interacting data, namely fitting power-laws as in the interacting case, is possible. The extracted exponents are shown in Fig. S3 together with the interacting data. We note that this evaluation is not physically motivated and hence the non-interacting exponents are not expected to be connected to any dynamical exponents. However, they do give insight into the extent of perceived slow relaxation in the absence of interactions. We observe that the non-interacting exponents reach their background value at much lower disorder strengths than in the interacting case. In addition, the background value is found to be lower, which is consistent with the saturation of $1/z$ observed in the interacting case (see Fig.4) being caused by background couplings, as such couplings affect the interacting system stronger than the non-interacting system [42, 43].

Interaction dependence of the power-law exponents

In this work, we performed the analysis of the interacting system at a fixed interaction strength of $U = 4\,J$. The value was chosen, since here we expect the strongest interaction shift of the MBL transition compared to the non-interacting localization transition [13]. Fig. S4 shows the extracted power-law exponents as a function of interaction strength at $\Delta = 2.5\,J$. We find that the exponent shows a behavior reminiscent of the interaction dependence observed in Ref. [13]: We find a maximum inter-

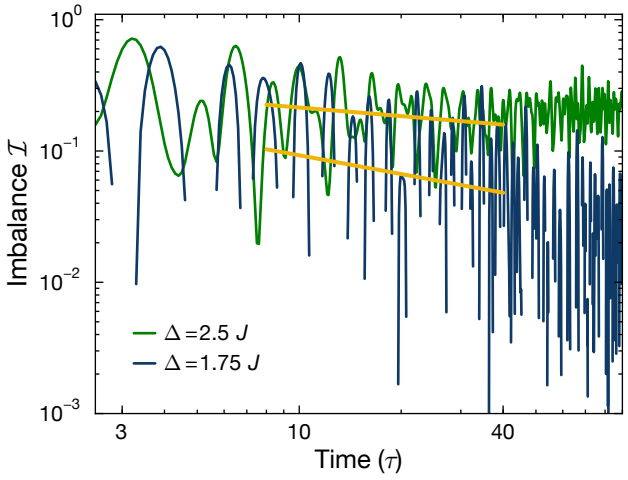

FIG. S2. **Simulation of non-interacting time traces:** Imbalance decay of an initial CDW of non-interacting particles for $\Delta = 1.75\,J$ and $\Delta = 2.5\,J$ on a system with 200 sites, averaged over 1000 phases ϕ. The fast initial decay of the imbalance from its starting value is omitted. We observe much stronger oscillations than in the experiment, but reproduce the general trend. This is illustrated by the yellow lines, which show fits to the *experimental* data on the timescales of the experiment.

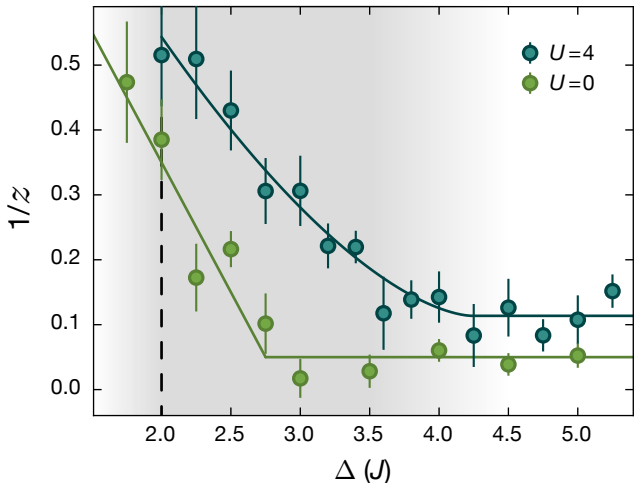

FIG. S3. **Naive noninteracting exponents:** Exponents of a power-law fit to the interacting and non-interacting time traces between $8 - 40\,\tau$. Errorbars denote the covariance error of the fit. Solid lines are guides-to-the-eye. We note that in the absence of interactions the Griffiths mechanism is not present and hence power-law fits are not physically motivated. In particular, the finite exponents visible for $\Delta/J = 2 - 3$ at $U = 0$ are remnants of the oscillating short-time dynamics (see Fig. S2) and are not expected to be related to any dynamical exponent.

action effect around $U = 5\,J$ and values approaching the non-interacting limit in the regime of hard core interactions. This is expected due to an exact mathematical mapping from hardcore fermions to free fermions in the absence of doubly occupied lattice sites [13].

Details of the experimental setup

We start our experiments by cooling an equal mixture of the two lowest lying hyperfine states (denoted as $|\uparrow\rangle$,$|\downarrow\rangle$) of ^{40}K atoms to a temperature of $0.15\,T/T_{\mathrm{F}}$ in a dipole trap, where T_{F} is the Fermi temperature. The cold gas is then loaded into a three dimensional optical lattice, where the formation of doublons is suppressed to below $\approx 8\%$ by strong repulsive interactions.

The optical lattice consists of two deep $\lambda_\perp \approx 738\,\mathrm{nm}$ lattices along the orthogonal directions at a strength of $40\,\mathrm{E}_{\mathrm{r}}^{\perp}$, creating an array of one-dimensional tubes. Here $E_r^i = \mathrm{h}^2/(2m\lambda_i^2)$ denotes the recoil energy, where λ_i is the respective lattice's wavelength and m is the mass of ^{40}K. In the tubes, we employ a primary $\lambda_p \approx 532\,\mathrm{nm}$ lattice, which is superimposed by a weaker, incommensurate $\lambda_d \approx 738.2\,\mathrm{nm}$ disorder lattice, to implement the Aubry-André model [38] with on-site interactions [36].

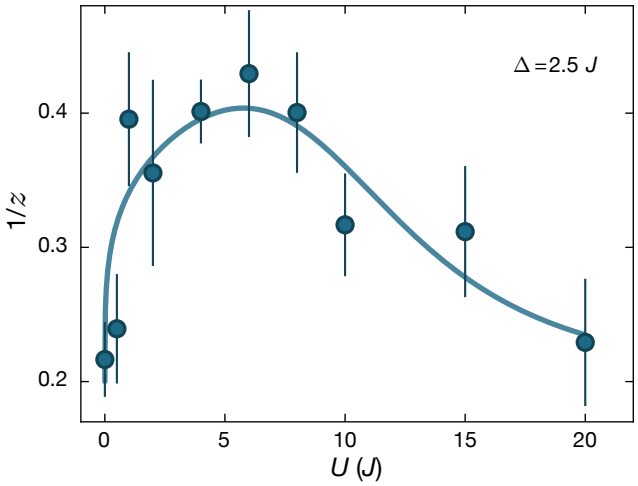

FIG. S4. **Power-law exponents versus interaction strength:** Fitted experimental exponents as a function of the interaction strength U at a disorder strength of $\Delta = 2.5\,J$. We note that in the absence of interactions the power-law exponent might not be well defined, as the dynamics are not expected to follow a power-law.

$$\begin{aligned}\hat{H} =& -J\sum_{j,\sigma}(\hat{c}^{\dagger}_{j+1,\sigma}\hat{c}_{j,\sigma} + \mathrm{h.c.}) \\ &+ \Delta\sum_{j,\sigma}\cos(2\pi\beta j + \phi)\hat{n}_{j,\sigma} + U\sum_{j}\hat{n}_{j,\uparrow}\hat{n}_{j,\downarrow},\end{aligned} \tag{S01}$$

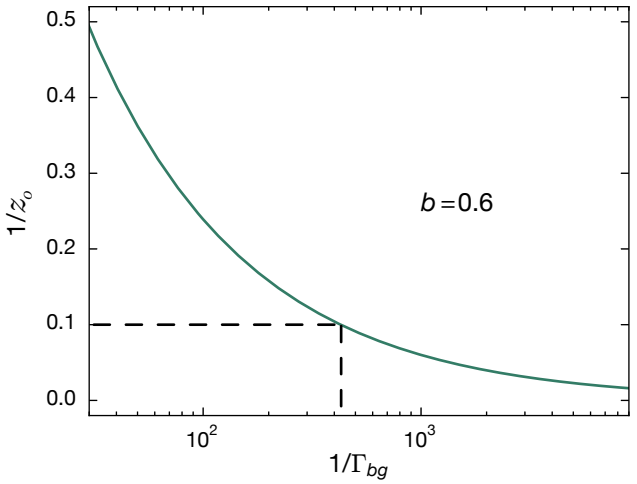

FIG. S5. **Effect of background decay:** Exponents extracted by a power-law fit in the experimental time window of $8-40\,\tau$ to a stretched exponential decay with rate Γ_{bg} and stretching exponent $b = 0.6$. The offset $z_o^{-1} \approx 0.1$ we find in Fig. 4 corresponds to a background decay with a lifetime of $1/\Gamma_{bg} \approx 400-500\,\tau$, as is indicated by the dashed lines.

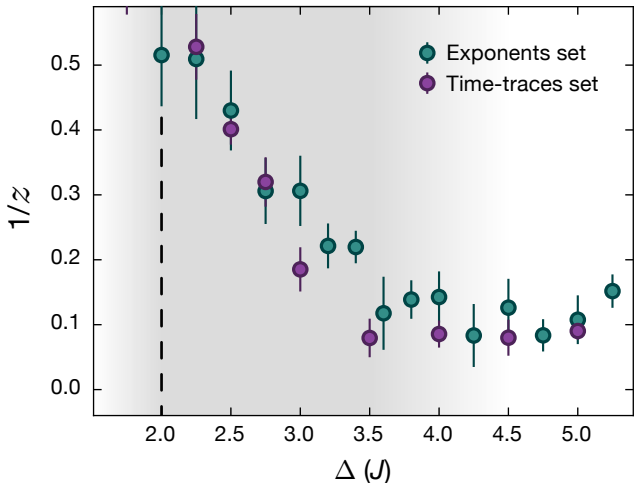

FIG. S6. **Power law exponent extracted from time traces in Fig. 3:** Exponents extracted from the dataset used in Fig. 3 (Time-traces set) and in Fig 4 (Exponents set).

The operators $\hat{c}^\dagger_{j,\sigma}$ and $\hat{c}_{j,\sigma}$ are the creation and annihilation operators for spin $\sigma \in \{|\uparrow\rangle, |\downarrow\rangle\}$ on site j, the respective number operators are given by $\hat{n}_{j,\uparrow}$ and $\hat{n}_{j,\downarrow}$. $J \approx \mathrm{h} \times 500\,\mathrm{Hz}$ denotes the tunneling rate in the primary lattice. The strength of the correlated disorder Δ and its phase ϕ is controlled by the depth and relative phase of the disorder lattice. The incommensurable ratio is given by $\beta = \lambda_d/\lambda_p$. Additionally, we achieve independent control of the interaction strength U via a Feshbach resonance centered around 202.1 G [50]. We note that there are small deviations between our setup and an ideal Aubry-Andreé model as, e.g. the disorder lattice not only modulates the on-site energies, but also the hopping rates by $\lesssim 10\%$. Details of these deviations can be found in Ref. [13].

We create the initial charge-density wave using an additional superlattice with respect to the primary lattice with $\lambda_l \approx 1064\,\mathrm{nm}$, by following the same loading procedure as in Ref. [13]. After the evolution time, the superlattice is employed again to extract the imbalance $\mathcal{I}$ via a band mapping technique [40].

Analysis of background decay

In the analysis of the power-law exponents (see Fig. 4) we find that at large Δ, the exponents saturate at a non-zero offset value z_0^{-1}. This behavior is consistent with an underlying exponential long-term decay $\mathcal{I}(t) \sim e^{-(\Gamma_{bg}t)^b}$ of the imbalance. Here, Γ_{bg} is the imbalance lifetime and b the stretching exponent. Such stretched exponential decays have been found to arise in our system due to external bath couplings [42, 43], such as photon scattering and residual tunnel couplings between the one dimensional tubes. Fig. S5 shows the result of fitting a power-law decay in the experimental time window of $8-40\,\tau$ to a stretched exponential decay with $b = 0.6$ (a value we often found in previous works [42, 43]) and various Γ_{bg}. We find, that the observed offset of our exponents z_o^{-1} corresponds to an imbalance lifetime of $1/\Gamma_{bg} \approx 400-500\,\tau$, which is consistent with previous results [42, 43].

Usage of two different sets of data

In this work we use two different sets of data for the exponents in Fig. 4 and the time-traces in Fig. 3. The two sets were taken under the same experimental conditions, but approximately half a year apart and are compared in Fig. S6. We find that the two sets agree within experimental noise. The two datasets were employed as one of them contains more disorder strengths while the other uses finer time steps.

Details of exact diagonalization simulations

We follow the time evolution of the wave-function $|\Psi(t)\rangle = \exp(-iH\tau)|\Psi(0)\rangle$ from an initial CDW state $|\Psi(0)\rangle$ in the Krylov space $\mathcal{K}_m(H, |\Psi(0)\rangle)$, using a parallel solver as implemented in the SLEPc library [51]. The time evolution is essentially exact, with a convergence ensured by using small times steps, $d\tau$ in between 0.1 and 1 (we set $J = 1$ in the simulations). We use chains of size $S = 12, S = 16$ and for some values of quasi-periodic potential $S = 20$, taking open boundary

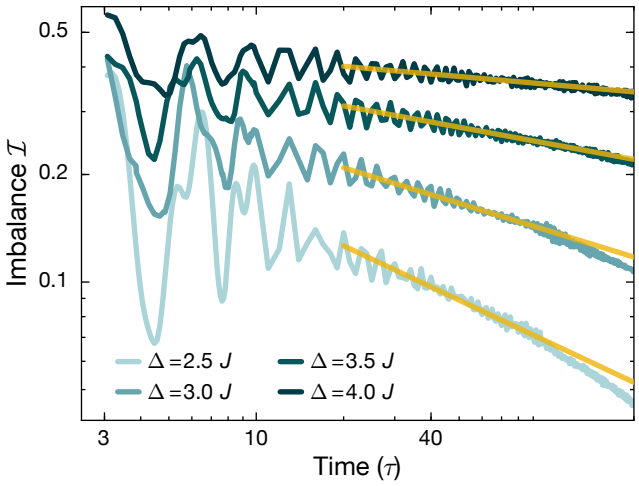

FIG. S7. **ED time traces:** Decay of an initial charge-density wave as simulated on systems with 16 sites and 8 atoms. Thickness of the lines denotes the statistical error after averaging over random initial conditions. The yellow lines illustrate fits to the data between $20-80\,\tau$, used to extract the exponents shown in Fig. 4. At longer times and for smaller values of disorder, a deviation from this power-law regime is observed, which might be attributed to a redistribution of atoms when parts of the system thermalize or a delocalized spin sector [47].

conditions and fixing $\beta = 0.721$. We work at zero magnetization and quarter-filling ($S/4$ up spin and $S/4$ down spin fermions) with Hilbert space sizes 48400 ($S = 12$), 3312400 ($S = 16$), and larger than 240 Millions ($S = 20$). The initial state is a product state chosen of CDW form, with a random repartition of up and down spins. We average results for the imbalance $\mathcal{I}(\tau) = \langle\Psi(\tau)|\mathcal{I}|\Psi(\tau)\rangle$ over between 80 and 200 combinations of initial states and random values of the phase ϕ (chosen uniformly in $[0, 2\pi]$). For the direct comparison to the experimental traces in Fig. 3, we scale the simulated imbalances by a factor of 0.9 to account for the independently measured initial imbalance in the experimental CDW state.

Fig. S7 shows exemplary traces, as well as the fitted power-laws. The fits have been performed between $20-80\,\tau$, as at shorter times the initial oscillations in the imbalance heavily affect the fit. In the experiment, this is not a problem, as the initial oscillations dephase quicker due to averaging over many 1D tubes with slightly different J [13]. We observe that the power-law fits describe the behavior well until the imbalance decay becomes steeper (at around $100\,\tau$ for the smaller disorder strengths). This might be due to a redistribution of atoms and spins resulting in a "melting" of rare regions and therefore a faster decay at later times. Such a redistribution could occur by parts of the system thermalizing or due to a delocalized spin sector [47]. However, understanding this regime will require additional work.

Fig. S8 shows time traces for $\Delta = 3\,J$ and system sizes of $S = 12, 16, 20$. We observe a slightly faster decay for larger system sizes. Due to the limited sizes available, we cannot extrapolate to infinite size. However, we find for all S investigated, a systematic decrease of $1/z$ with increasing the disorder strength. For Fig. 3 and 4, in order to perform simulations for a larger set of disorder values, we used $S = 16$. We estimate the finite size error of the exponents indicated in Fig. 4 as the difference between the result of the $S = 12$ and the $S = 16$ sites simulation. We find that this error decreases with increasing disorder strength. However, in the regime of large disorder ($\Delta \gtrsim 4J$) close to the transition, where the correlation length diverges, we cannot reach long enough times and large enough S to correctly estimate $1/z$, resulting in an estimate of the error on the exponent of the order of the exponent $1/z \approx 0.04$ itself.

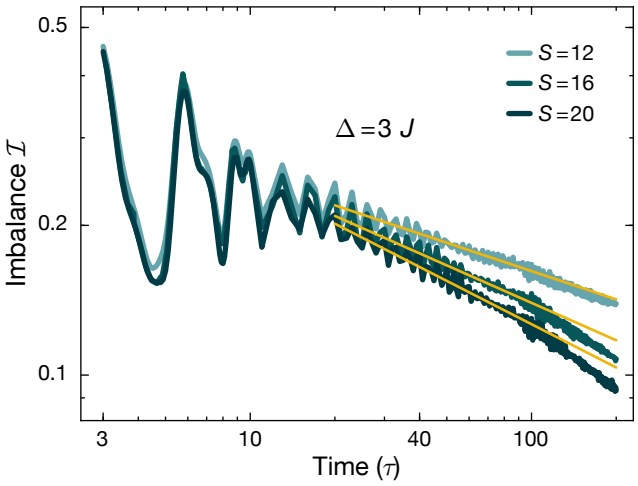

FIG. S8. **Size dependence of ED traces:** Time evolution of the imbalance for various system sizes at $\Delta = 3\,J$ and $U = 4\,J$. Thickness of the lines denotes the statistical error after averaging over random initial conditions. Yellow lines indicate power-law fits between $20-80\,\tau$. We find a faster decay for larger system sizes.